Princeton Plasma Physics Laboratory

PPPL- 5010
PPPL- 5010

Runaway Generation In Disruptions Of Plasmas in TFTR

E.D. Fredrickson, M.G. Bell, G. Taylor and S.S. Medley

MARCH, 2014

PRINCETON PLASMA PHYSICS LABORATORY

Prepared for the U.S. Department of Energy under Contract DE-AC02-09CH11466.

Runaway Generation in Disruptions of Plasmas in TFTR

E. D. Fredrickson, M. G. Bell, G. Taylor, S. S. Medley
Princeton Plasma Physics Laboratory, Princeton, New Jersey

Abstract

Many disruptions in the Tokamak Fusion Test Reactor (TFTR) [D. Meade and the TFTR Group, in *Proceedings of the International Conference on Plasma Physics and Controlled Nuclear Fusion, Washington, DC, 1990* (International Atomic Energy Agency, Vienna, 1991), Vol. 1, pp. 9–24] produced populations of runaway electrons which carried a significant fraction of the original plasma current. In this paper, we describe experiments where, following a disruption of a low-beta, reversed shear plasma, currents of up to 1 MA carried mainly by runaway electrons were controlled and then ramped down to near zero using the ohmic transformer. In the longer lasting runaway plasmas, Parail-Pogutse instabilities were observed.

I. Introduction

Major disruptions of tokamak plasmas, which result in the abrupt termination of plasma current, have been a problem throughout the history of tokamaks. As tokamaks become larger and the stored energy and current increase, the danger from disruptions increases [1,2]. First, the initial loss of confinement deposits the plasma kinetic energy on plasma facing components (PFCs) on millisecond timescales which can damage their surfaces. Second, the rapid decay of the poloidal magnetic field induces large currents, and thus forces, in vacuum vessel components. In addition, if the toroidal electric field induced during the current quench exceeds the Dreicer field [3], electrons in the plasma can be accelerated in one collision time, or mean free path, to a velocity where the collisional drag is less than the accelerating force. These electrons become runaway electrons as they continue to accelerate [4,5]. The runaway problem is exacerbated for higher current devices, such as ITER, because an avalanching process can rapidly amplify any small seed current of runaways [4,5,6] via direct collisions. In devices as large as ITER, the runaway beams can contain enough energy to jeopardize internal components of the machine [1].

In disruptions of high performance plasmas on TFTR [7], the plasma kinetic energy was lost on a timescale of order 100 μs during the initial thermal quench, and the magnetic energy then decayed on a timescale of order 10 ms. Many disruptions on TFTR generated a substantial runaway population, evidenced by a burst of hard x-rays coincident with a plateau, or pause, in the current quench. Typically this current plateau lasted only a few tens of milliseconds.

The rapid drop in plasma beta and internal inductance during the thermal quench mean that the plasma is no longer in radial force equilibrium. The response of the plasma equilibrium to the disruption depends on details of of the poloidal field coils, their power supplies and the feedback control system. However, on the sub-millisecond timescale of the thermal quench, the externally applied vertical (major axial) field maintaining radial equilibrium is essentially constant. With the collapse of the force on the plasma in the outward major radius direction due to its kinetic pressure, the plasma shifts radially inwards onto the inner "bumper" limiter. This is illustrated for a representative disruption in Fig. 1. The plasma current begins to drop following the disruption, but has a short plateau at about 400kA (Fig. 1a) indicating the presence of runaway electrons. During the initial current drop, the one-turn loop voltage reaches 200V, or ≈10V/m (Fig. 1b). The plasma major radius begins to decrease following the thermal quench until the plasma is pushed entirely onto the inboard limiter which is at a radius of 1.65m (Fig. 1c). As the plasma is pushed onto the bumper limiter, the nascent runaway beam is "scraped off" onto the limiter, creating a burst of hard x-rays (Fig. 1d).

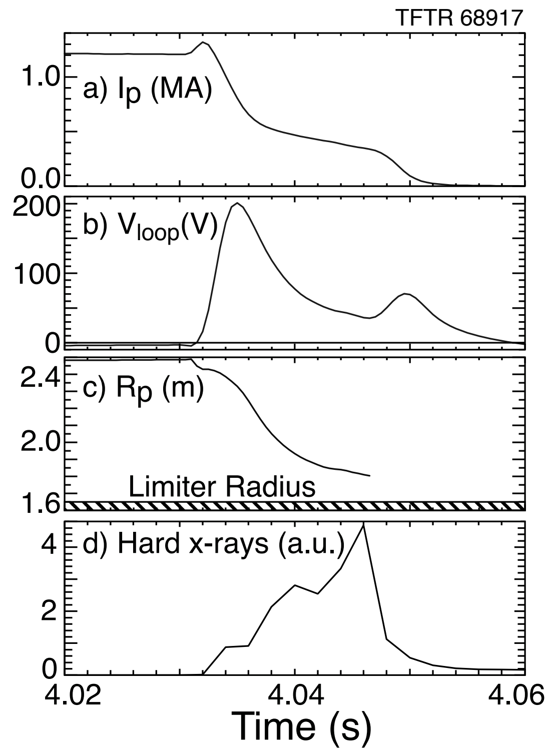

Fig. 1. Disruption during rampdown of a 2.5MA plasma, a) plasma current with short runaway plateau, b) surface 1-turn voltage, c) major radius of the center of the plasma boundary (limiter radius indicated by hash marks), and d) hard x-ray emission.

The ability of next step, ignited fusion devices, with 100's of MJ of magnetic energy readily converted to runaways during a disruption, to survive such events is a major engineering design challenge. There is a research effort underway internationally to develop techniques for avoiding disruptions, or suppressing runaway production if disruptions could not be avoided. Post-disruption runaway electron plasmas have been studied on many devices including JT-60U [7-9], JET [10-15], Tore Supra [16] and TEXTOR. Experiments to develop the techniques needed for control of the runaway plasma in shaped tokamaks are underway on the DIII-D tokamak [17]. Here we present the possibility that such runaway plasmas may be controlled, and the energy in the runaway electrons slowly extracted. We present the available data on these controlled runaway discharges from the TFTR experiment and present some limited experimental data on events that resemble Parail-Pogutse instabilities [18,19].

The plasma illustrated in Fig. 1 was a high-current discharge with normal (*i.e.* positive) magnetic shear throughout and a high internal inductance. In what follows, we will examine runaway plasmas created during experiments with low inductance, hollow current profiles. Under these conditions of low β and low plasma inductance at the time of the disruption, the change in equilibrium from the pre-disruption plasma to the post disruption runaway plasma was sufficiently small that the runaway discharge remained reasonably centered within the vacuum chamber. In these cases, runaway plasmas were maintained for as long as 4 s.

The plasma current in TFTR was controlled by feedback to a programmed waveform and the control system was designed to execute a shutdown procedure if the plasma current deviated by more than a preset amount from this programmed value, as would generally occur during a disruption at the start of the current quench. The negative loop voltage applied by the central solenoid to reduce the total plasma current in response to the disruption, also reduced the energy in the runaway electrons.

II Experimental results

Here we discuss disruptions in a class of TFTR plasmas characterized by negative magnetic shear in the core, commonly referred to as 'reversed shear' or 'enhanced reversed shear' plasmas [20]. During the current rise of these plasmas, the plasma beta and internal inductance were low enough that the radial position control system on TFTR was able to regain control of the plasma radial position after the thermal quench and magnetic reconnection event to prevent the runaways from being scraped off onto the bumper limiter. In these post-disruption plasmas, up to 70% of the original plasma current was carried by runaways. The

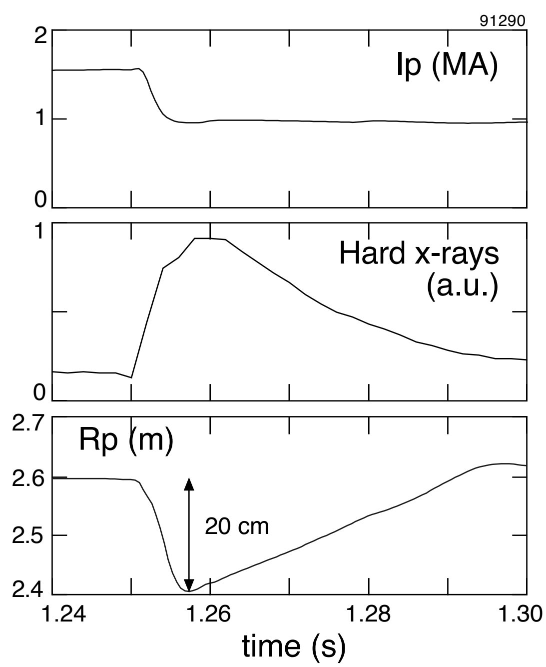

Fig. 2. Disruption of a reversed shear plasma, a) plasma current with run-away tail, b) hard x-rays, c) plasma major radius.

runaway current was held in equilibrium while the current was slowly ramped down over a period of several seconds. The control and then slow ramp down of the runaway current following a major disruption is a potentially attractive scenario for ITER because, although a significant fraction of the magnetic energy may be converted to runaways, that energy can then be extracted by the transformer. The creation of a substantial runaway current, rather than complete termination of the original plasma current, reduces the flux change responsible for inducing eddy current forces on machine components.

In Fig. 2 are shown traces from a representative disruption of this type of plasma. There is a only a weak positive current spike preceding the disruption as the initial reconnection does not decrease the plasma inductance substantially for current profiles that are flat or hollow. The loss of beta does result in a brief inward shift of the plasma, but the initial shift is only ≈ 20% of the minor radius, and within 30ms the feedback system restores the plasma to its programmed position. Hard x-ray emission peaks at about the time the plasma movement is arrested, consistent with the interpretation that the hard x-rays result from runaway electrons being 'scraped off' on the bumper limiter. When the plasma begins moving away from the limiter, the runaways can be confined and hard x-ray emission decreases. In this case the initial 1.6 MA discharge becomes a 1 MA runaway-dominated discharge.

There were no measurements of the electron temperature profile evolution through the runaway generation phase and thus there is uncertainty in the modeling of the runaway generation process. Reasonable estimates suggest, however, that the Rosenbluth avalanche process is not required to generate the 1MA of runaway current in this discharge, although it may play a role. The runaway distribution would be generated in the first few ms following the disruption, after which

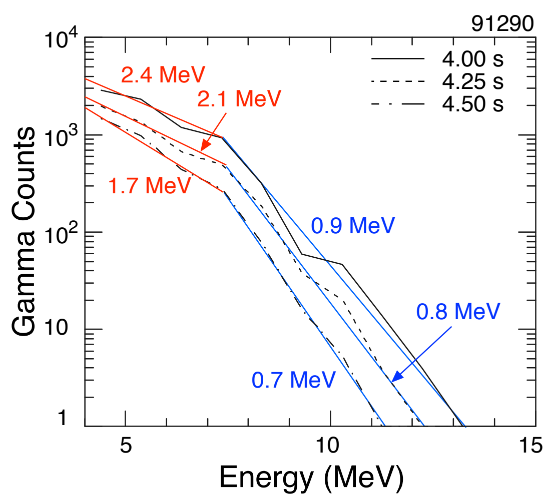

Fig. 3. Energy spectrum of gammas from lost runaway electrons showing a roughly exponential dependence on energy at three times during the runaway tail. The numbers indicate the gradient scale-length of the exponential fall-off with energy. Spectra displayed show counts in 30ms bins (raw data is in 1 ms bins).

the loop voltage drops near zero.

A gamma ray spectrometer [21-24] provided information on the distribution of the runaway energies. The energy spectrum of the gammas is shown in Fig. 3 at three times during the runaway phase. The spectrum can be fit with exponentials above and below a threshold energy: below 8 MeV $n_{counts} \approx exp(-E/T_{gamma})$, $T_{gamma} \approx 2.1$ MeV ± 0.3 MeV and for energies above 8 MeV $T_{gamma} \approx 0.8$ MeV ± 0.1 MeV.

The relation of the gamma energy spectrum to the runaway energy spectrum is complicated [25-27]. The distribution of runaway electrons is expected to have an exponential dependence on energy, $n_{ra} \approx exp(-W/T_{ra})$ [4-6] and for an avalanching distribution of runaways, $T_{ra} \approx (17 + 3.4Z)$ MeV [6]. The relatively low characteristic energies T_{ra} observed in this case suggest that either avalanching physics is not responsible for maintaining this part of the runaway distribution, or perhaps losses of high energy runaways are determining the spectral shape. A more extensive reconstruction of the runaway distribution from the gamma spectrum [27] might help clarify some of these issues, but that is beyond the scope of this paper.

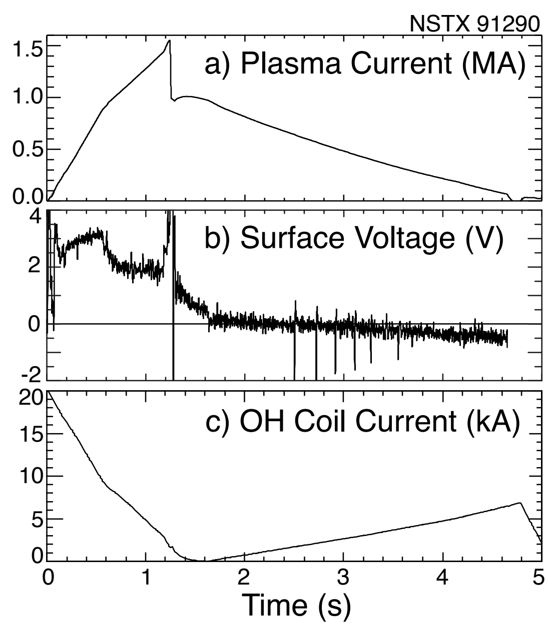

Fig. 4. Decay of runaway tail, a) plasma current, b) surface voltage, and c) OH coil current.

The evolution of this runaway discharge on a longer timescale is shown in Fig. 4. The runaway current decays roughly linearly, persisting for 3.7s after the disruption. In this case, where the disruption occurred before the reversal of the central solenoid current, the control system and power supplies responded by applying a continuing positive ramp to the solenoid current until the plasma current was reduced to zero when the power supply was turned off. The resulting *negative* loop voltage reduced the runaway current. The ≈ 1.5 V expected from the increasing solenoid current is nearly cancelled by the estimated inductive voltage of ≈ 1.5 V from the plasma current ramp down, consistent with a surface-voltage of ≈ 0 within experimental uncertainty. This implies that the resistive losses in the plasma are negligible, supporting the assumption that the plasma current is being carried by runaway electrons. This scenario was common for disruptions which occurred during the early phase of reversed shear plasmas.

III. Runaway instabilities

The spikes visible in the surface voltage starting at 2.5s in Fig. 4b suggest the excitation of Parail-Pogutse instabilities in the runaway electron beam [28-30]. Fig. 5 shows time traces of the electron cyclotron emission (ECE), the plasma internal inductance, the surface voltage, the radiated power and the D-alpha emission, all undergoing perturbations simultaneously. The strong bursts of ECE suggest that the tail instabilities scatter the runaway electrons from predominantly parallel motion into motion perpendicular to the magnetic field and the sudden increase in perpendicular energy results in a burst of ECE. The internal inductance decreases at each instability burst, reflected in the negative voltage spikes, indicating that the current profile broadens. The Parail-Pogutse instability, involving velocity scattering that converts parallel to perpendicular energy, is likely to be playing an important role here, both limiting the maximum velocity of the runaways and removing energy and current-carrying runaways from the plasma. The changes in the internal inductance l_i are consistent with broadening of the current profile at the Parail-Pogutse burst and after the burst the electrons accelerate in the core and peak the current profile again, increasing l_i.

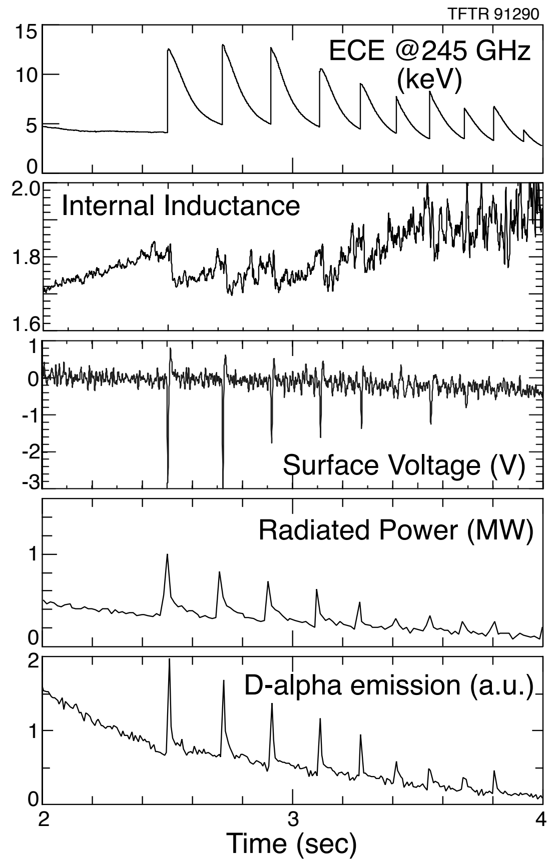

Fig. 5. a) ECE radiation temperature, b) internal inductance, c) surface voltage, d) radiated power, e) D-alpha emission.

The spikes in radiated power and D_α emission suggest that energy is deposited on plasma facing components, but whether that energy is in the form of radiation, lost runaways or thermal plasma is not clear.

Spectra of electron cyclotron emission measured with a scanning X-mode Michelson interferometer [31] are shown in Fig. 6. The spectrum is shown before (solid line) and shortly after the peak of the burst (dashed line). The (non-relativistic) frequency ranges of the first, second and third ECE harmonics are shown at the top of the figure, with first harmonic emission from the outboard plasma edge being at ≈100GHz.

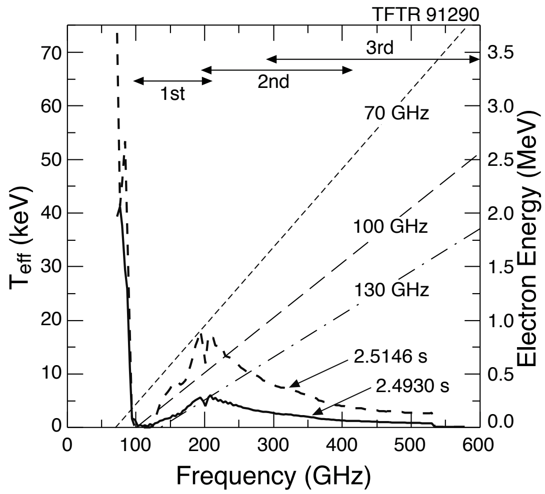

Fig. 6. Spectrum of ECE measured with the X-mode Michelson interferometer. The solid trace is the emission spectrum preceding the ECE burst, the broken trace at the peak of the ECE burst. The three dashed lines indicate the electron energy needed to downshift the emission to the indicated frequency. The frequency ranges at the top indicate the *unshifted* range of 1st, 2nd and 3rd harmonic emission across the plasma midplane.

A feature similar to that seen below 100 GHz in Fig. 6 was seen during NBI heated "supershot" discharges after extensive lithium coating had been applied to the TFTR limiter [32]. In those plasmas a narrow-frequency emission peak was seen below the fundamental, at a frequency corresponding to the upper hybrid frequency at the plasma outer edge. It was speculated that this might represent a super-radiant maser phenomenon. If this were the case here, it would help to explain the gap in the spectrum. However, those supershot plasmas had higher density and did not have runaways in the core.

Interpretation of the electron cyclotron emission from a relativistic plasma is difficult [33-36]. However the intense emission bursts are likely to be relativistically down-shifted emission from runaways in the plasma core, with the lowest frequency emission being the most down-shifted, *i.e*. from the most energetic runaway electrons. For the X-mode emission, the first harmonic should be weak, and the emission below 200 GHz probably represents relativistically down-shifted 2nd harmonic emission. The dashed lines indicate the electron energy needed to downshift the emission to the indicated frequency. Thus, emission downshifted from 200 GHz to 130 GHz would correspond to an electron energy of about 0.26 MeV.

The upper panel of Fig. 7 shows data digitized at 500 kHz during one of the ECE bursts. These data are from the grating polychromator ECE diagnostic [37] for the lowest and highest frequencies covered by the instrument. The timescale for the increase in emission is 50-100 μs at 210 GHz, but of order 200 μs at 250 GHz. The emission then decays on a timescale of ≈ 80ms. This probably represents the timescale for the decay in the perpendicular energy of the scattered electrons, which is not maintained by the (parallel) loop voltage. The density profiles as measured with the multi-chord interferometer before and after the ECE burst are shown in the lower panel of Fig. 7. The density increases by ≈ 20% on axis, although the 10 ms time resolution of this measurement cannot resolve the details of this rise. Although these densities should give optical thicknesses >1 for electron temperatures >50 eV over the plasma cross-section, the optical depth may not be sufficient to prevent some burn-through of the intense, down-shifted ECE.

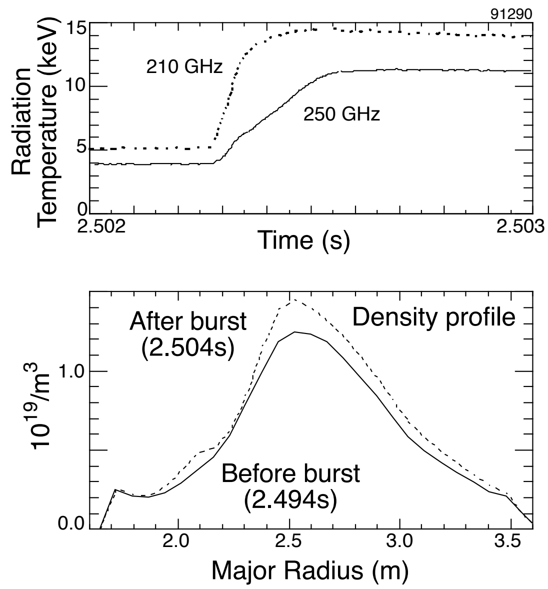

Fig. 7. a) Electron cyclotron emission from Grating Polychromator, b) density profiles reconstructed from the ten-channel interferometer.

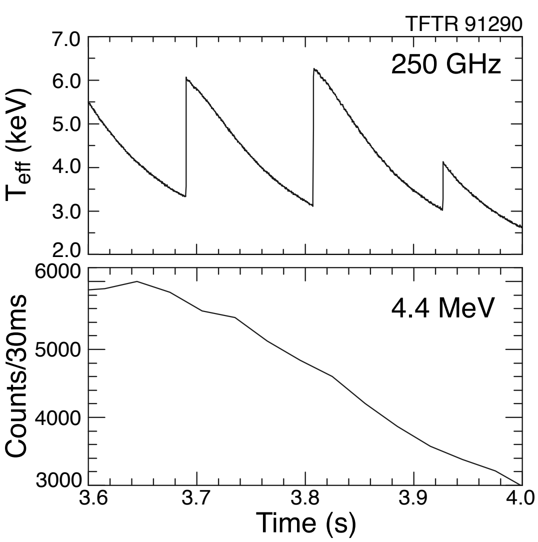

Fig. 8. a) Effective temperature from ECE emission showing inverted sawteeth at each tail instability event, b) hard x-ray or gamma emission at 4.4 MeV showing no effect of instabilities.

It may be assumed that the decay of the ECE following the Parail-Pogutse instability represents the decay of the perpendicular energy component of the energetic electrons scattered from parallel by the Parail-Pogutse instability. The decay could result from collisional drag, cyclotron emission or further pitch-angle scattering. The collisional velocity slowing-down time on the electrons can be estimated as [38]:

$\tau_{slow} \approx 1.3x10^5 E^{3/2}/(n_e \lambda_{ee})$

where n_e is the electron density per cm^3, E is the runaway energy in eV, and λ_{ee} is the coulomb logarithms for electron-electron and electron-ion collisions. Using a range of densities from Fig. 7b ($0.7x10^{19}/m^3$ to $1.3x10^{19}/m^3$) and runaway energies from 100 keV up to 300 keV gives velocity slowing down times between 20 ms and 190 ms, which can be compared with the ≈ 80 ms decay time for ECE emission. A full simulation of the evolution of the energetic electron population evolution, and resulting electron cyclotron emission is beyond the scope of this paper, however, these estimates suggest that the ECE decay rate following Parail-Pogutse instabilities is roughly consistent with the expected collisional slowing down time for runaways with energies roughly between 100 keV and 300 keV. No evidence of the Parail-Pogutse instabilities is seen in the gamma spectrum for energies above 4.4 MeV (Fig. 8), suggesting that only runaway electrons with energies below this are affected by the instabilities.

At each instability burst, there are spikes in the radiated power and the D_α emission. This is consistent with a loss to the plasma facing components of energetic electrons at each burst as the tail instability scatters the runaway electrons radially. The transient power losses can be significant with radiated power spikes of up to 0.5 MW observed, which, integrated over the burst width of about 40 ms, corresponds to ≈ 20 kJ. The number of runaways may be estimated from the total current. To carry 1 MA, it would take ≈ $3.4x10^{17}$ relativistic electrons. If the average energy of a runaway electron (from the exponential distribution) is $T_{ra} \approx 4$ MeV, then the total energy in the runaway beam may be very approximately estimated as ≈ 200 kJ. Thus ≈ 10% of the energy in the runaway tail could be lost at each burst.

Summary

These experimental results from TFTR demonstrate the possibility of controlling the runaway current generated following disruptions. In TFTR, more than 60% of the initial 1.6 MA of plasma current could be converted to runaways. Measurements of the gamma ray energy spectra suggest an exponential distribution in energy for the runaways. In low-beta reversed-shear discharges, the equilibrium of the post-disruption runaway plasma was well controlled and the runaway electron current could then be ramped down over several seconds using the central transformer solenoid. A periodic instability was seen in the runaway plasma, consistent with the model proposed by Parail and Pogutse. The instability apparently pitch-angle scattered the runaways, resulting in large increases in the electron cyclotron emission. Coincident with the instabilities, spikes in the radiated power up to 0.5 MW were seen in the bolometer signal and the internal inductance, deduced from magnetic measurements, decreased, indicating an outward redistribution of the runaway current, with concomitant negative voltage spikes.

Acknowledgements

We would like to express our appreciation to the TFTR team, with special thanks for T. Carroll, L. Nixon, R. Reed, and C. Scimeca for support in recovering TFTR data. This work was supported under U.S. DoE contract Nos. DE-AC02-76CH03073 and DE-AC02-09CH11466.

Bibliography

[1] Chapter 3: MHD stability, operational limits and disruptions, T.C. Hender, J.C Wesley, J. Bialek, A. Bondeson, A.H. Boozer, R.J. Buttery, A. Garofalo, T.P Goodman, R.S. Granetz6, Y. Gribov, O. Gruber, M. Gryaznevich, G. Giruzzi, S. Gu ¨nter8, N. Hayashi, P. Helander, C.C. Hegna, D.F. Howel, D.A. Humphreys, G.T.A. Huysmans, A.W. Hyatt, A. Isayama, S.C. Jardin, Y. Kawano, A. Kellman, C. Kessel1, H.R. Koslowski, R.J. La Haye, E. Lazzaro, Y.Q. Liu, V. Lukash, J. Manickam, S. Medvedev, V. Mertens, S.V. Mirnov, Y. Nakamura, G. Navratil, M. Okabayashi, T. Ozeki, R. Paccagnella, G. Pautasso, F. Porcelli, V.D. Pustovitov, V. Riccardo, M. Sato, O. Sauter, M.J. Schaffer, M. Shimada, P. Sonato, E.J. Strait, M. Sugihara, M. Takechi, A.D. Turnbull E. Westerhof, D.G. Whyte, R. Yoshino, H. Zohm and the ITPA MHD, Disruption and Magnetic Control Topical Group, Nucl. Fusion **47** (2007) S128

[2] *Impurity control and material physics*, M. Ulrickson, J. N. Brooks, H. F. Dylla, R. J. Goldston, J. R. Haines, D. N. Hill, R. A. Langley, G. H. Neilson, and K. L. Wilson, Fusion Technology **21** (1992) 1279.

Theory of runaway electrons

[3] H. Dreicer, Phys. Rev. 115, 238 (1959); 117, 239 (1960).

[4] H. H. Fleischmann, S. J. Zweben, "*Evaluation of potential runaway generation in large-tokamak disruptions*", PPPL report 2914 (1993),

[5] R. Jayakumar, H. H. Flieschmann, S. J. Zweben, "*Collisional avalanche exponentiation of runaway electrons in electrified plasmas*", Phys. Rev. A **172** (1993) 447.

[6] M.N. Rosenbluth, S.V. Putvinski "T*heory for avalanche of runaway electrons in tokamaks*", Nucl. Fusion **37**, 1355 (1997).

[7] D. Meade and the TFTR Group, in *Proceedings of the International Conference on Plasma Physics and Controlled Nuclear Fusion, Washington, DC, 1990* (International Atomic Energy Agency, Vienna, 1991), Vol. 1, pp. 9–24.

JT-60U

[7] *The softening of current quenches in JT-60U,* Yoshino, R., Neyatani, Y, M., Hosogane, N, S.W. Wolfe, M. Matsukawa, H. Ninomiya, Nucl. Fusion **33**, (1993) 1599.

[8] *Generation and termination of runaway electrons at major disruptions in JT-60U*, R. Yoshino, S. Tokuda,Y. Kawano, Nucl. Fusion **39** (1999) 151.

[9] *Runaway electrons in magnetic turbulence and runaway current termination in tokamak discharges*, R. Yoshino, S. Tokuda Nucl. Fusion **40** (2000) 1293.

JET

[10] *Generation and loss of runaway electrons following disruptions in JET*, R.D. Gill, Nucl. Fusion **33** (1993) 1613.

[11] *Direct observations of runaway electrons during disruptions in the JET tokamak,* R.D. Gill, B. Alper, A.W. Edwards, L.C. Ingesson, M.F. Johnson, D.J. Ward, Nucl. Fusion **40** (2000) 163.

[12] *Behaviour of disruption generated runaways in JET*, R.D. Gill, B. Alper, M. de Baar, T. C. Hender, M.F. Johnson, V. Riccardo and contributors to the EFDA-JET Workprogramme, Nucl. Fusion **42** (2002) 1039

[13] *Damping of relativistic electron beams by synchrotron radiation*, F. Andersson, P. Helander, L.-G. Eriksson, Phys. Plasmas **8** (2001) 5221.

[14] *Study of runaway electron generation during major disruptions in JET*, V.V. Plyusnin, V. Riccardo, R. Jaspers, B. Alper, V.G. Kiptily, J. Mlynar, S. Popovichev, E. de La Luna, F. Andersson and JET EFDA contributors, Nucl. Fusion **46** (2006) 277

[15] *Runaway generation during disruptions in JET and TEXTOR,* M. Lehnen, S.S. Abdullaev, G. Arnoux, S.A. Bozhenkov, M.W. Jakubowski, R. Jaspers, V.V. Plyusnin, V. Riccardo, U. Samm, JET EFDA Contributors, The TEXTOR Team, Journal of Nuclear Materials **390–391** (2009) 740–746

Tore Supra

[16] *Control of runaway electron beam heat loads on Tore Supra*, F.Saint-Laurent, J. Bucalossi, C. Reux, S. Bremond, D. Douai, C. Gil, P. Moreau, 38th EPS Conference on Plasma Physics (2011) paper O3.118.

TEXTOR

[] M. Forster et al Nucl. Fusion **52** (2012) 083016.

[] K.H. Finken et al Nucl. Fusion **30** (1990) 859.

DIII-D

[17] *Control of post-disruption runaway electron beams in DIII-D*, N. W. Eidietis, N. Commaux, E. M. Hollmann, D. A. Humphreys, T. C. Jernigan, R. A. Moyer, E. J. Strait, M. A. VanZeeland, J. C. Wesley, and J. H. Yu, Phys. Plasmas **19**, 056109 (2012)

Parail-Pogutse

[18] *The kinetic theory of runaway electron beam instability in a tokamak*, V.V. Parail, O.P. Pogutse, Nucl. Fusion **18** (1978) 303.

[19] V.V. Parail and O.P. Pogutse "Runaway electrons in a tokamak", in Reviews of Plasma Physics, V.11 (Kadomtsev, B.B., Ed.) Consultants Bureau, New York (1986).

Enhanced Reversed Shear

[20] *Improved Confinement with Reversed Magnetic Shear in TFTR*, F.M. Levinton, M.C.Zarnstorff, S.H.Batha, M. Bell, R.E. Bell, R.V. Budny, C. Bush, Z. Chang, E. Fredrickson, A. Janos, J. Manickam, A. Ramsey, S. A. Sabbagh, G. L. Schmidt, E.J. Synakowski, and G. Taylor, Phys. Rev. Lett. **75** (1995) 4417.

Gamma detector

[21] *Fusion Gamma Diagnostics* S. S. Medley, Rev. Sci. Instrum. **56** (1988) 975.

[22] F.E. Cecil and S.S. Medley, "Gamma ray measurements during deuterium and ^{3}He discharges on TFTR", Nucl., Instrum. and Methods **271** (1988) 628.

[23] *Performance of the fusion gamma diagnostic on TFTR*, S. S. Medley, S. D. Scott, A. L. Roquemore, F. E. Cecil, Rev. Sci. Instrum. **61** (1990) 3226.

[24] *Absolute Calibration of fusion gamma ray detector on TFTR*, S. S. Medley, A. L. Roquemore, F. E. Cecil, Rev. Sci. Instrum. **63** (1992) 4857.

Reconstruction of runaway distributions

[25] *Modelling of the electron distribution based on bremsstrahlung emission during lower-hybrid current drive on PLT*, J. Stevens, S. von Goeler, S. Bernebei, M. Bitter, T.K. Chu, P. Efthimion, N. Fisch, W. Hooke, J. Hosea, F. Jobes, C. Karney, E. Meservey, R. Motley, G. Taylor, Nucl. Fusion **25** (1985) 1529.

[26] *Angular distribution of the bremsstrahlung emission during lower hybrid current drive on PLT*, S. von Goeler, J. Stevens, S. Bernebei, M. Bitter, T.K. Chu, P. Efthimion, N. Fisch, W. Hooke, K. Hill, J. Hosea, F. Jobes, C. Karney, J. Mervine, E. Meservey, R. Motley, P. Roney, S. Sesnic, K. Silber, G. Taylor, Nucl. Fusion **25** (1985) 1515.

[27] *Reconstruction of distribution functions of fast ions and runaway electrons in fusion plasmas using gamma-ray spectrometry with applications to ITER,* A.E. Shevelev, E.M. Khilkevitch, V.G. Kiptily, I.N. Chugunov, D.B. Gin1, D.N. Doinikov, V.O. Naidenov, A.E. Litvinov, I.A. Polunovskii and JET-EFDA Contributors, Nucl. Fusion **53** (2013) 123004.

Exp. PP instabilities

[28] *Analysis of Electron Cyclotron Emission from non-thermal Discharges in ASDEX Tokamak*, D.J. Campbell, A. Eberhagen, S.E. Kissel, Nucl. Fusion **24** (1984) 297.

[29] *Analysis of the Parail-Pogutse instability in the presence of lower hybrid and electron cyclotron waves*, D. Farina, M. Lontano, Nucl. Fusion **26** (1986) 1733.

[30] S. von Goeler, J. Stevens,, C. Karney, S. Bernabei, M, Bitter, T.K. Chu, P. Efthimion, K, Hill, W. Hooke, F. Jobes, E. Mazzucato, E. Meservev, R. Motley, P. Roney, N. Sauthoff, S. Sesnic, G. Taylor, F. Tenney, E. Valeo, "*Determination of the Electron Velocity Distribution from the Soft and Hard x-ray Emission During Lower-hybrid Current Drive on PLT*", PPPL report 2012 (June 1983)

ECE diagnostics

[31] *Broadband measurement of electron cyclotron emission in TFTR using a quasioptical light collection system and a polarizing Michelson interferometer*, F. Stauffer, D. A. Boyd, R. C. Cutler, M. Diesso, M. P. McCarthy, J. Montague and R. Rocco, Rev. Sci. Intr. **59** 2139 (1988).

[32] G. Taylor, D. K. Mansfield, Nucl. Fusion **38** 1819 (1998).

[33] Cavallo, A., Cutler, R. C., and McCarthy, M. P., Rev. of Sci. Instr. **59** (1988) 889.

ECE measurements

[34] *Absorption of cyclotron waves at down-shifted frequencies by an energetic electron tail in the PLT tokamak*, E. Mazzucato, P. Efthimion, Nucl. Fusion **25** (1985) 1681.

[35] K. Kato and I. Hutchinson, Phys. Rev. Lett. **56**, 340 (1986).

[36] S. Preische, P. C. Efthimion, and S. Kaye, Phys. Plasmas **3** 4065 (1996).

[37] *Oblique electron cyclotron emission for electron distribution studies*, S. Preische, P.C. Efthimion, S. M. Kaye, Rev. Sci. Instrum. **68** 409 (1997).

slowing down time

[38] J. D. Huba, NRL Plasma Formulary, Naval Research Laboratory, Washington DC, NRL/PU/6790--09-523, 2009, p. 32.

The Princeton Plasma Physics Laboratory is operated
by Princeton University under contract
with the U.S. Department of Energy.

Information Services
Princeton Plasma Physics Laboratory
P.O. Box 451
Princeton, NJ 08543

Phone: 609-243-2245
Fax: 609-243-2751
e-mail: pppl_info@pppl.gov
Internet Address: http://www.pppl.gov